

Reduction of primordial chaos by generic quantum effects

Martin Bojowald,^{1*} David Brizuela,^{2†} Paula Calizaya Cabrera^{3‡} and Sara F. Uria^{2§}

¹ Institute for Gravitation and the Cosmos, The Pennsylvania State University,
104 Davey Lab, University Park, PA 16802, USA

² Department of Physics and EHU Quantum Center, University of the Basque Country
UPV/EHU, Barrio Sarriena s/n, 48940 Leioa, Spain

³ Department of Physics & Astronomy, Louisiana State University,
Baton Rouge, LA 70803, USA

Abstract

According to general relativity, the generic early-universe dynamics is chaotic. Various quantum-gravity effects have been suggested that may change this behavior in different ways. Here, it is shown how key mathematical properties of the classical dynamics can be extended to evolving quantum states using quasiclassical methods, making it possible to apply the established dynamical-systems approach to chaos even to quantum evolution. As a result, it is found that quantum fluctuations contribute to the reduction of the primordial chaos in early-universe models.

A powerful statement about the complicated nature of the primordial state of the universe is made by generic features of chaotic dynamics in classical descriptions based on general relativity [1, 2]. The evolving anisotropy of space in the early, high-curvature universe can be described by an effective potential that encodes the effects of space-time curvature by walls that restrict the anisotropy parameters to a finite region. Mathematical results about billiard dynamics applied to these walls, which happen to be convex and therefore defocusing, then guarantee chaos [3]. Quantum effects, such as fluctuations or various geometrical implications of approaches to quantum gravity, may be expected to make this behavior even more counter-intuitive and harder to unravel. Finding reliable knowledge of the initial state of the universe could then be impossible.

In particular, a long series of studies in supergravity and string theory has confirmed this expectation to some degree, showing that the dynamics remains chaotic [4, 5] when extra dimensions and fields relevant for unification are included. Such new ingredients extend the classical configuration space of anisotropy parameters for the universe by including new independent degrees of freedom. Nevertheless, they come along with their own curvature contributions that share qualitative features of the walls in the effective anisotropy potential, maintaining the classical chaotic dynamics. These models, however, are not fully

*email address: bojowald@psu.edu

†email address: david.brizuela@ehu.eus

‡email address: pcaliz1@lsu.edu

§email address: sara.fernandezu@ehu.eus

quantum because they do not consider states with fluctuations and correlations obeying uncertainty relations.

Independently, quantum cosmology with fluctuating states has also been applied to this question, but so far with mixed results [6, 7, 8, 9], owing for instance to the difficult task of evaluating dynamical properties of the quantum wave function of a single universe. The large number of degrees of freedom contained in a quantum wave function, compared with the corresponding classical degrees of freedom, makes it hard to disentangle different, potentially competing, dynamical features. Specific properties are therefore identified in these approaches that may reduce chaos, such as by isotropization or bounded curvature. These effects may help to avoid the strong anisotropy potential that implies chaos in the classical dynamics, but they do not directly confront it.

Here, we apply a systematic quasiclassical expansion to quantum cosmology and provide the first generic example of a suppression of chaos in primordial cosmology, based on general features of quantum fluctuations. This new result relies on a minimal inclusion of quantum effects that implement the spread-out nature of quantum states along classical trajectories. It should therefore be present in any model of quantum gravity because it does not require specific assumptions about the nature of quantum space-time.

To this end, we derive a new effective potential that extends the classical anisotropy potential into a higher-dimensional quasiclassical configuration space in which the classical anisotropy parameters are accompanied by fluctuation degrees of freedom that also parameterize higher moments of an evolving quantum state. This description makes it possible to retain the appealing geometrical picture of billiard models [5], also extended by new degrees of freedom, but with a specific modification of the classical walls that has not been considered before. (Related methods have recently been applied to individual reflections in the anisotropy potential [10].) At the same time, established methods from dynamical-systems theory can be applied in the quasiclassical description in order to analyze detailed quantitative properties of the primordial chaos. While chaos is not completely removed, its strength is noticeably reduced.

Following the Belinskii–Khalatnikov–Lifshitz (BKL) scenario [1], the high-curvature dynamics close to the big bang can be studied by analyzing a spatially homogeneous space-time model with line element

$$ds^2 = -N^2(t)dt^2 + \sum_{i=1}^3 a_i^2(t)\sigma_i^2, \quad (1)$$

where $N(t)$ is the lapse function, σ_i , with $i = 1, 2, 3$, form a basis of differential forms on the manifold of the rotation group $SO(3)$, parameterized for instance by Euler angles, and $a_i(t)$ are three independent functions of time. As the $a_i(t)$ change at different rates, the anisotropy of the universe evolves, while space expands if the product $a_1(t)a_2(t)a_3(t)$ increases. The approach to the big-bang singularity can be studied by inverting the direction of time.

It is useful to separate the changing size of space from the evolution of its anisotropy, which can conveniently be achieved by introducing Misner variables [2]: The expansion

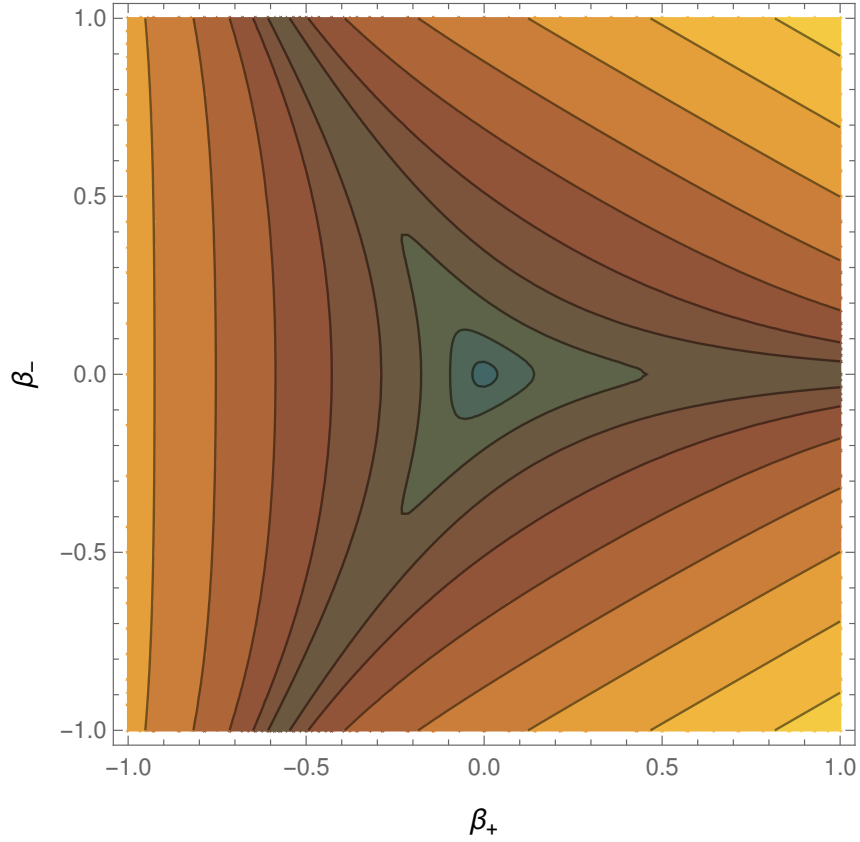


Figure 1: Contour plot of the classical anisotropy potential (5).

rate is described logarithmically by a real parameter

$$\alpha = \frac{1}{3} \ln(a_1 a_2 a_3), \quad (2)$$

such that the big-bang singularity is approached for $\alpha \rightarrow -\infty$. The two remaining degrees of freedom independent of α are the anisotropy parameters

$$\beta_+ = \frac{1}{6} \ln(a_1 a_2 / a_3^2) \quad \text{and} \quad \beta_- = \frac{1}{2\sqrt{3}} \ln(a_1 / a_2). \quad (3)$$

General relativity implies that the dynamics of α and β_{\pm} in a universe with line element (1) is described by the expression

$$\mathcal{C} = \frac{1}{2} e^{-3\alpha} (-p_\alpha^2 + p_-^2 + p_+^2) + e^\alpha V(\beta_+, \beta_-) = 0, \quad (4)$$

with the anisotropy potential

$$V(\beta_+, \beta_-) := \frac{1}{6} \left[e^{-8\beta_+} + 2e^{4\beta_+} \left(\cosh(4\sqrt{3}\beta_-) - 1 \right) - 4e^{-2\beta_+} \cosh(2\sqrt{3}\beta_-) \right]. \quad (5)$$

(The simple coefficients in the quadratic momentum dependence are a consequence of the choice of defining (3).)

The expression \mathcal{C} defined in (4) serves as a Hamiltonian constraint: It imposes an energy-balance constraint by being required to vanish, and, at the same time, it generates Hamilton's equations for α , β_{\pm} , and their momenta $p_{\alpha} := -\frac{e^{3\alpha}}{N} \frac{d\alpha}{dt}$ and $p_{\pm} := \frac{e^{3\alpha}}{N} \frac{d\beta_{\pm}}{dt}$. Since α changes monotonically and we are interested in the dynamics of β_{\pm} during expansion or contraction, we can solve the constraint equation (4) for

$$H := -p_{\alpha} = \sqrt{p_+^2 + p_-^2 + 2e^{4\alpha}V(\beta_+, \beta_-)}, \quad (6)$$

and view it as the Hamilton function (no longer constrained to vanish) for β_{\pm} and their momenta evolving with respect to α . The dynamics is then determined by the 2-dimensional motion in the anisotropy potential (5). It has steep exponential walls for large anisotropy and a triangular symmetry that can best be seen by looking at the contour plot in Fig. 1.

Note that in (6) this potential is multiplied by a factor of $e^{4\alpha}$. The potential walls therefore shrink close to the singularity, giving room for larger anisotropy. The dynamics of β_{\pm} is characterized by a sequence of reflections at the potential walls. As shown by Fig. 1, these walls are always convex. General mathematical results can then be invoked to conclude that the dynamics of anisotropies is chaotic.

Previous results that suggested a reduction or disappearance of chaos exploited possible ways to tear down the walls of the anisotropy potential, for instance by using modified dynamics that isotropizes the evolution or limits the values of curvature and therefore the height of the walls. A problematic aspect of such modified dynamics is that it would also undermine the BKL scenario, which in classical general relativity justifies the application of a spatially homogeneous geometry close to any (spacelike) singularity. Our new quantum effect does not tear down the walls, but rather, as we will show, reshapes them by making them partially concave. Concave and therefore focusing walls may or may not imply chaos [11]. According to our dedicated analysis of the new system encountered here, the strength of chaos is reduced by a certain degree depending on how much concavity is included.

As already commented above, the walls are reshaped by quantum effects. Heuristically, a wave function on the anisotropy plane with coordinates β_{\pm} is spread out and the corners of the triangular region are therefore washed out, partially closing them off by concave caps. In order to make this precise, we have to be able to derive a sufficiently general effective potential that retains the geometrical picture of the classical model even while it includes quantum effects. Since the anisotropy parameters may change rapidly when curvature is large, the quantum potential should be able to capture non-adiabatic effects, ruling out standard methods such as low-energy effective potentials or other derivative expansions. As we will show, the expected effect is described well by quasiclassical methods based on a parameterization of states by moments.

We will consider only quantum states of the anisotropy parameters and their momenta, and therefore include the central moments

$$\Delta(\beta_+^i \beta_-^j p_+^k p_-^l) := \langle (\hat{\beta}_+ - \beta_+)^i (\hat{\beta}_- - \beta_-)^j (\hat{p}_+ - p_+)^k (\hat{p}_- - p_-)^l \rangle_{\text{Weyl}}, \quad (7)$$

in completely symmetric or Weyl ordering. The dynamics of a state described by the moments is governed by a Hamilton operator quantizing (4). Its expectation value $\langle \hat{\mathcal{C}} \rangle$, taken in a state described by (7), is a function of the moments, for which a series expansion can be obtained if the anisotropy potential is first expanded in a Taylor series. As in (6), a square root then defines the effective Hamiltonian H_Q with respect to α :

$$H_Q^2 = \langle \hat{H}^2(\hat{\beta}_+, \hat{\beta}_-, \hat{p}_+, \hat{p}_-) \rangle = p_+^2 + \Delta(p_+^2) + p_-^2 + \Delta(p_-^2) + e^{4\alpha} \sum_{i,j=0}^{+\infty} \frac{1}{i!j!} \frac{\partial^{i+j} V(\beta_+, \beta_-)}{\partial \beta_+^i \partial \beta_-^j} \Delta(\beta_+^i \beta_-^j). \quad (8)$$

To simplify the notation, here and from now on we refer to expectation values by their classical names, $\beta_{\pm} = \langle \hat{\beta}_{\pm} \rangle$ and $p_{\pm} = \langle \hat{p}_{\pm} \rangle$.

By keeping the moments as independent degrees of freedom, in addition to the expectation values β_{\pm} and p_{\pm} , we are able to capture non-adiabatic effects in which moments may change rapidly compared with the corresponding classical degrees of freedom. In the anisotropy potential of relevance here, such rapid changes may happen when a state gets squeezed into the corners of the triangular potential, precisely where we expect spread-out wave functions to introduce concave components to the walls. However, keeping all the moments independent takes us from a 2-dimensional configuration plane to an infinite-dimensional space. For tractability, we have to find a compromise in which some moment degrees of freedom are kept independent while most of them are strictly related to the independent ones. An example is a Gaussian approximation, in which the expectation values and a fluctuation parameter s are free, while all other moments are specific functions of s .

The quasiclassical formulation is open to studies of different classes of states, defined through specific relationships between the moments. Our main interest here is to analyze a succession of reflections at steep walls, which (unlike, say, tunneling) is expected to preserve the shape of a wave packet. Moments of a single wave packet, such as Gaussian one in which we have two independent fluctuation parameters, s_{\pm} for β_{\pm} , should therefore be reliable. Anisotropy moments are then defined as

$$\Delta(\beta_+^{2n} \beta_-^{2m}) = \frac{s_+^{2n} s_-^{2m}}{2^n 2^m} \frac{(2n)!(2m)!}{n!m!}. \quad (9)$$

The Hamiltonian also contains the momentum terms p_{\pm}^2 , which, in an expectation value, imply fluctuation terms: $\langle \hat{p}_{\pm}^2 \rangle = p_{\pm}^2 + \Delta(p_{\pm}^2)$. In order to obtain a standard dynamical system, we should express the momentum fluctuations $\Delta(p_{\pm}^2)$ in terms of momenta $p_{s_{\pm}}$ canonically conjugate to the anisotropy parameters s_{\pm} . Methods from Poisson geometry, which relate the quantum commutator of operators to a Poisson bracket of their expectation values [12, 13, 14], show that momentum fluctuations expressed in terms of fluctuation momenta must be such that

$$\Delta(\beta_{\pm} p_{\pm}) = s_{\pm} p_{s_{\pm}} \quad , \quad \Delta(p_{\pm}^2) = p_{s_{\pm}}^2 + \frac{U_{\pm}}{s_{\pm}^2}, \quad (10)$$

where $U_{\pm} = \Delta(p_{\pm}^2) \Delta(\beta_{\pm}^2) - \Delta(\beta_{\pm} p_{\pm})^2 \geq \hbar^2/4$ determines saturation properties of the state. Similar parameterizations have been used in a variety of fields [15, 16, 17, 18].

To conclude this part of our construction, the quantum anisotropy potential in the 4-dimensional space with coordinates β_{\pm} and s_{\pm} receives two types of new terms: (i) repulsive potentials U_{\pm}/s_{\pm}^2 from the kinetic energy operator, which prevent the fluctuation parameters from reaching zero and thereby enforce uncertainty relations, and (ii) a series expansion in s_{\pm} that follows from replacing (8) with (9). In fact, after inserting the parametrization of the moments (9), this series can be summed up explicitly, resulting in the extended anisotropy potential

$$V_Q(\beta_+, \beta_-, s_+, s_-) \quad (11)$$

$$= \frac{1}{6} \left[e^{-8\beta_+ + 32s_+^2} + 2e^{4\beta_+ + 8s_+^2} \left(e^{24s_-^2} \cosh(4\sqrt{3}\beta_-) - 1 \right) - 4e^{-2\beta_+ + 2s_+^2 + 6s_-^2} \cosh(2\sqrt{3}\beta_-) \right].$$

The 4-dimensional nature of the new configuration space complicates our heuristic arguments because the expected concave caps around the triangular corners of the classical potential depend on which 2-dimensional cross-section we consider. Nevertheless, a crucial difference implied by non-zero s_{\pm} can be seen by considering, for instance, the cross-section defined by $\beta_- = 0$. The classical potential is then reduced to the simple function $6V(\beta_+, 0) = e^{-8\beta_+} - 4e^{-2\beta_+}$. The two exponentially decreasing terms illustrate the steep exponential wall on the left of Fig. 1, which approaches zero on the right where the confined region is stretched out into a narrow channel. The extended potential, evaluated on the same cross-section, implies the reduced potential

$$6V_Q(\beta_+, 0, s_+, s_-) = e^{-8\beta_+ + 32s_+^2} - 4e^{-2\beta_+ + 2s_+^2 + 6s_-^2} + 2e^{4\beta_+ + 8s_+^2} \left(e^{24s_-^2} - 1 \right), \quad (12)$$

in which an exponentially increasing function contributes as well. Since s_- cannot be zero, owing to the U_-/s_-^2 term in the Hamiltonian, even a small value will eventually lead to the increasing $\exp(4\beta_+)$ to dominate for positive β_+ . The classical channel has thus been closed off, which requires a concave contribution to the walls. (In fact, for large s_- , almost the entire wall would become concave; see App. A.) Actually, this is a generic feature for any quantum state since the operator $(\cosh(4\sqrt{3}\hat{\beta}_-) - 1)$, which multiplies $\exp(4\hat{\beta}_+)$ in the potential (5), is positive definite; see App. B. Therefore, in the effective potential, $\langle \exp(4\hat{\beta}_+) (\cosh(4\sqrt{3}\hat{\beta}_-) - 1) \rangle$ produces a dominant exponential contribution for large β_+ , regardless of the value of β_- , which closes the classical channel on the right corner. Similar arguments can be applied to the other two classical channels located at $\beta_- = \pm\sqrt{3}\beta_+$.

Since the 4-dimensional dynamics in the extended anisotropy potential (11) is given by a dynamical system in canonical form, its properties of chaos can be unambiguously analyzed. Details of such an analysis are presented in Ref. [23], and we note that the two main methods that have been used in the past to derive coordinate-independent properties of chaos agree in that quasiclassical effects lead to a reduction of its degree. First, there exists a canonical transformation that maps our 4-dimensional dynamical system to motion within a finite region of a 4-dimensional space with constant negative curvature, generalizing a crucial property of the Misner–Chitre transformation [19] used in [20] to

conclude that all Lyapunov exponents are positive. The quasiclassical dynamics therefore remains chaotic.

Secondly, a quantitative measure of chaos can be obtained from the fractal dimension of subsets of different dynamical outcomes in the space of initial values [21, 22]. Here, three different outcomes are naturally defined by which of the three corners in the classical anisotropy plane will be approached first, a definition that can also be used in the quasiclassical potential.

In our analysis, we have chosen 160 different sets of initial data for the quantum variables $(s_{\pm}, p_{\pm}, U_{\pm})$, and divide the space of initial data in corresponding outcomes. For our sample, the dimension of the boundary between different regions has been computed to be in the range [1.21, 1.58], depending on the specific initial values of the quantum variables, while the classical repeller has a fractal dimension of 1.86 (see Ref. [23] for more details). Therefore, in all the analyzed cases, quantum fluctuations decrease this dimension, which implies a reduction of the chaotic behavior. This can be clearly seen in Fig. 2, where the fractal picture is smoothed out in the quantum case. In particular, specific details of the reduction depend on quantum-information properties of the primordial state of the universe.

Acknowledgements

DB and SFU thank, respectively, the Max-Planck-Institut für Gravitationsphysik and The Pennsylvania State University for hospitality while part of this work was done. SFU was funded by an FPU fellowship and a mobility scholarship of the Spanish Ministry of Universities. This work was supported in part by NSF grant PHY-2206591, the Alexander von Humboldt Foundation, the Basque Government Grant IT1628-22, and by the Grant PID2021-123226NB-I00 (funded by MCIN/AEI/10.13039/501100011033 and by “ERDF A way of making Europe”).

A Turn-over from convex to concave

For simplicity, let us analyze the convexity of the wall around the corner to the right of the trapped region (see Fig. 1). This wall is described by the term

$$W(\beta_+, \beta_-, s_-) = e^{4\beta_+} \left(e^{24s_-^2} \cosh(4\sqrt{3}\beta_-) - 1 \right),$$

because the other terms in the effective potential (11) decrease exponentially for large β_+ . Convexity of the wall means that the gradient vector of W , which is normal to constant- W surfaces, has a decreasing angle with the β_+ -axis as β_- increases. A straightforward calculation determines this angle θ through

$$\tan \theta = \sqrt{3} \frac{\sinh(4\sqrt{3}\beta_-)}{\cosh(4\sqrt{3}\beta_-) - e^{-24s_-^2}}.$$

Hence, the wall is convex while $\partial \tan \theta / \partial \beta_- < 0$. For the classical model ($s_- = 0$), this is always the case, which, as mentioned, is an indicator of chaos. However, once that quantum effects are taken into account, some parts of the wall become concave. In particular, it turns into concave behavior when

$$\frac{\partial \tan \theta}{\partial \beta_-} = 12 \frac{1 - e^{-24s_-^2} \cosh(4\sqrt{3}\beta_-)}{(\cosh(4\sqrt{3}\beta_-) - e^{-24s_-^2})^2} = 0,$$

at which point we have

$$\tan \theta = \frac{\sqrt{3}}{\sqrt{1 - e^{-48s_-^2}}}.$$

For large s_- , this turn-over point takes place at $\tan \theta = \sqrt{3}$, or $\theta = 60^\circ$, that is, just about the middle of the wall.

B State-independent closure of corners

Here we prove that the corners of the classical potential are closed off in any effective potential, not only for the quantum states with high-order moments parameterized by (9).

We first demonstrate the strict inequality $\langle \cosh(4\sqrt{3}\hat{\beta}_-) \rangle > 1$ for any state of our model quantized on the Hilbert space $L^2(\mathbb{R}^2, d\beta_+ d\beta_-)$. Using the β -representation of wave functions $\psi(\beta_+, \beta_-)$, we conclude that the operator $\sinh^2(4\sqrt{3}\hat{\beta}_-)$ is positive definite because there is no (normalizable) state in which $\langle \sinh^2(4\sqrt{3}\hat{\beta}_-) \rangle = 0$, which can be seen on the spectral decomposition of $\hat{\beta}_-$: On the spectrum, the operator $\sinh^2(4\sqrt{3}\hat{\beta}_-)$ takes positive values unless $\beta_- = 0$. Since the spectrum is continuous, there is no normalizable state solely supported on this value, and therefore $\langle \sinh^2(4\sqrt{3}\hat{\beta}_-) \rangle$ cannot be zero.

Then, since $\sinh^2(4\sqrt{3}\hat{\beta}_-) = \cosh^2(4\sqrt{3}\hat{\beta}_-) - 1 = (\cosh(4\sqrt{3}\hat{\beta}_-) - 1)(\cosh(4\sqrt{3}\hat{\beta}_-) + 1)$, and $\cosh(4\sqrt{3}\hat{\beta}_-) + 1$ is also positive definite, $\cosh(4\sqrt{3}\hat{\beta}_-) - 1$ must be positive definite as well. Therefore, $\langle \cosh(4\sqrt{3}\hat{\beta}_-) \rangle > 1$ in any state.

We now apply this result to a generic effective potential obtained by taking the expectation value of a quantized (5) in some family of states, with high-order moments not necessarily parameterized by (9). Since $e^{4\hat{\beta}_+}$ and $\cosh(4\sqrt{3}\hat{\beta}_-) - 1$ are two commuting positive definite operators, their product is positive definite. Therefore, $\langle e^{4\hat{\beta}_+}(\cosh(4\sqrt{3}\hat{\beta}_-) - 1) \rangle$ cannot be zero. The corresponding reduced potential, defined as in (12), then always retains a contribution from the term $e^{4\hat{\beta}_+}(\cosh(4\sqrt{3}\hat{\beta}_-) - 1)$, which is unbounded in β_+ , and implies an exponential wall for any family of states with increasing β_+ , irrespective of the value of β_- . This is in contrast with the classical case, for which this term exactly vanishes at the axis $\beta_- = 0$, and, since the remaining terms in the classical potential decrease with β_+ , the classical exit channel on the right corner of Fig. 1 is open.

The reduced potential (12) is an explicit expression obtained for states red with moments parameterized by (9), but its crucial feature remains valid for any family of states. By means of symmetry, the same argument can be applied for the remaining two corners $\beta_- = \pm\sqrt{3}\beta_+$.

References

- [1] V. A. Belinskii, I. M. Khalatnikov, and E. M. Lifschitz, *Adv. Phys.* **31**, 639 (1982).
- [2] C. W. Misner, *Phys. Rev. Lett.* **22**, 1071 (1969).
- [3] Y. G. Sinai, *Russian Mathematical Surveys* **25**, 137 (1970).
- [4] T. Damour and M. Henneaux, *Phys. Rev. Lett.* **85**, 920 (2000), hep-th/0003139.
- [5] T. Damour, M. Henneaux, and H. Nicolai, *Class. Quantum Grav.* **20**, R145 (2003), hep-th/0212256.
- [6] A. Coley, *Class. Quantum Grav.* **19**, L45 (2002), hep-th/0110117.
- [7] M. Bojowald and G. Date, *Phys. Rev. Lett.* **92**, 071302 (2004), gr-qc/0311003.
- [8] H. Bergeron, E. Czuchry, J. P. Gazeau, P. Małkiewicz, and W. Piechocki, *Phys. Rev. D* **92**, 061302 (2015), arXiv:1501.02174.
- [9] G. Montani, M. V. Battisti, R. Benini, and G. Imponente, *Int. J. Mod. Phys. A* **23**, 2353 (2008), arXiv:0712.3008.
- [10] D. Brizuela and S. F. Uria, *Phys. Rev. D* **106**, 064051 (2022), arXiv:2207.00566.
- [11] L. A. Bunimovich, *Mathematical USSR Sbornik* **95**, 49 (1974).
- [12] M. Bojowald and A. Skirzewski, *Rev. Math. Phys.* **18**, 713 (2006), math-ph/0511043.
- [13] M. Bojowald and A. Skirzewski, *Int. J. Geom. Meth. Mod. Phys.* **4**, 25 (2007), hep-th/0606232, proceedings of “Current Mathematical Topics in Gravitation and Cosmology” (42nd Karpacz Winter School of Theoretical Physics), Ed. Borowiec, A. and Francaviglia, M.
- [14] B. Baytaş, M. Bojowald, and S. Crowe, *Phys. Rev. A* **99**, 042114 (2019), arXiv:1811.00505.
- [15] R. Jackiw and A. Kerman, *Phys. Lett. A* **71**, 158 (1979).
- [16] A. K. Pattanayak and W. C. Schieve, *Phys. Rev. Lett.* **72**, 2855 (1994), chaosdyn/9404001.
- [17] O. Prezhdo, *Theor. Chem. Acc.* **116**, 206 (2006).
- [18] T. Vachaspati and G. Zahariade, *Phys. Rev. D* **98**, 065002 (2018), arXiv:1806.05196.
- [19] D. M. Chitre, Ph.D. thesis, University of Maryland, College Park, 1972.
- [20] R. Benini and G. Montani, *Phys. Rev. D* **70**, 103527 (2004), gr-qc/0411044.

- [21] S. W. McDonald, C. Grebogi, E. Ott, and J. A. Yorke, *Physica D: Nonlinear Phenomena* **17**, 125 (1985).
- [22] N. J. Cornish and J. J. Levin, *Phys. Rev. D* **55**, 7489 (1997), gr-qc/9612066.
- [23] M. Bojowald, D. Brizuela, P. Calizaya Cabrera, and S. F. Uria, arXiv:2307.00063.

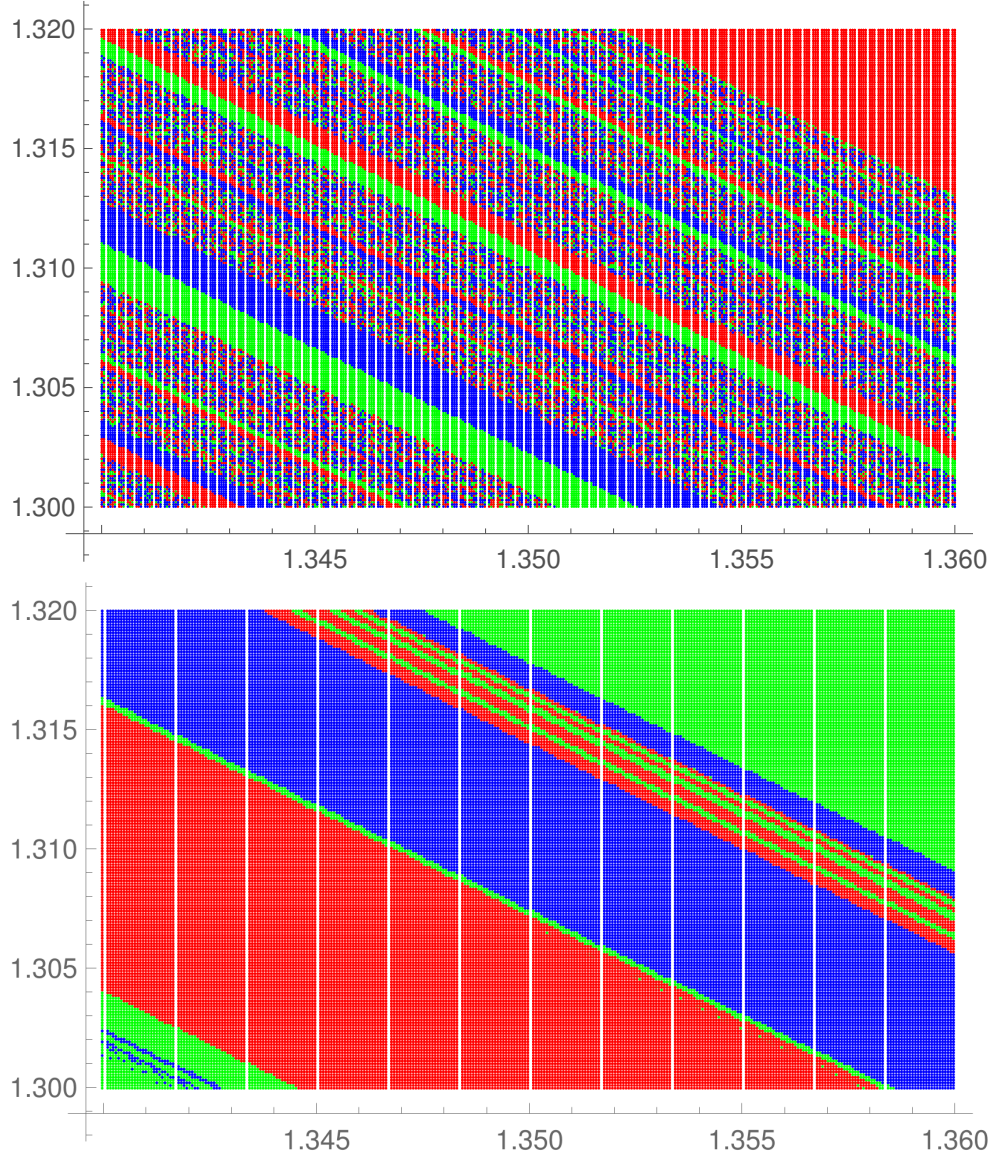


Figure 2: Subsets of three outcomes in a plane of initial values of the anisotropies, classical (top) and quasiclassical (bottom). Each color (red, blue, and green) stands for the corner of the potential that the corresponding point hits first.